GEOPHYSICAL RESEARCH LETTERS, VOL. ???, XXXX, DOI:10.1029/,

A solar terminator wave in thermospheric wind and density simultaneously observed by CHAMP

Huixin Liu

Research Institute for Sustainable Humanosphere, Kyoto University, Japan

Hermann Lühr

Helmholtz Centre Potsdam, GFZ German Research Centre for Geosciences, Potsdam, Germany

Shigeto Watanabe

Earth and Planetary Science Division, Hokkaido University, Japan

H. Liu, Research Institute for Sustainable Humanosphere, Kyoto University, Uji 611-0011, Japan (huixin@rish.kyoto-u.ac.jp)

H. Lühr, Helmholtz Centre Potsdam, GFZ German Research Centre for Geosciences, D-14473 Potsdam, Germany

S. Watanabe, Earth and Planetary Science Division, Hokkaido University, Sapporo 060-0810, Japan (huixin@ep.sci.hokudai.ac.jp)

A solar terminator wave has been revealed in thermospheric wind and density simultaneously observed by CHAMP. The wind terminator wave is out of phase with the density terminator wave. But both have wavefronts about 30° inclined to the terminator line at low latitudes, and wavelengths ranging between 3000-5000 km. They show a clear dawn-dusk asymmetry, with more pronounced wave signatures forming at dusk. Terminator wave is indiscernible in the dawnside wind. Most wave structures are observed at night, with some extension to the sunlit region around solstices. The midnight density maximum is seen to be closely connected to terminator wave structures, hence indicating a possible role of terminator waves in its formation.

1. Introduction

The solar terminator (ST) is the boundary between day and night. It represents a region of sharp change in the energy input from the solar radiation, which consequently leads to strong gradients in the Earth's atmosphere and ionosphere. In the vicinity of the solar terminator, the atmospheric gas is in a non-equilibrium state, giving rise to atmospheric irregularities and inhomogeneities [*Somsikov*, 1995; *Somsikov and Ganguly*, 1995]. Furthermore, the solar terminator tranverses through the atmosphere as the Earth rotates. This movement can generate atmospheric waves, as first pointed out by *Beer* [1973]. Theoretical formulations for the wave generation in the atmosphere and ionosphere have been treated in great details by *Beer* [1978], *Cot and Teitelbaum* [1980], and *Somsikov* [1987, 1995]. Using an atmospheric general circulation model extending from ground to exobase, *Fujiwara and Miyoshi* [2006] predicted ST-generated waves in the neutral temperature, composition, and meridional wind. Being a regular and global phenomenon, the moving terminator distinguishes itself from other wave generation sources as a stable, repetitive and predictable source.

Some of the above theoretical predictions have found their experimental evidences. For instance, solar terminator-excited waves in the ionosphere have been reported in a number of studies using various types of ionospheric sounding observations including also the GPS-TEC measurements [e.g. *Galushko et al.*, 1998; *Hocke and Igarashi*, 2002]. Though being much less reported, terminator waves in the thermosphere density have recently been revealed by *Forbes et al.* [2008] using data from the accelerometer experiment on board the CHAMP satellite. Since the thermospheric density and wind are, at first order, closely related to each other via the pressure gradient, it is reasonable to speculate a terminator wave to exist in the neutral wind as well.

To investigate this speculation from the perspective of observations, we utilize simultaneous neutral wind and density measurements from the CHAMP satellite.

2. Methodology and Data Selection

The near-circular, polar-orbiting satellite CHAMP was launched on July 15, 2000 to $\sim$456 km altitude. Its orbital plane drifts through all local times every 130 days. The tri-axial accelerometer on board yields estimates of thermospheric mass density and zonal wind, with respective accuracy of about 6×10^{-14} kg m^{-3} and 20 ms^{-1}. Details of the derivation procedure and related errors have been documented in *Liu et al.* [2005, 2006]. The sample rate is 0.1 Hz (Level 2 data), corresponding to a horizontal resolution of $\sim$70 km.

Our analysis here is based on simultaneous CHAMP measurements of thermospheric density and zonal wind during the period of 2002-2004 ($F10.7 \approx 90 - 250$). Only data under geomagnetic quiet conditions (Kp$\leq$3) are used to limit effects from geomagnetic disturbances. All density data have been normalized to a common altitude of 400 km and a common solar flux level of F10.7=150 using the NRLMSISE-00 model. This normalization facilitates better examination of local time and latitudinal variations by eliminating density variations due to orbit height and solar cycle. The zonal wind is not normalized, in view that it does not vary significantly with altitude above 300 km [*Wharton et al.*, 1984].

To possibly capture ST-generated wave structures in thermospheric wind and density, we calculate residuals of these quantities by subtracting a 3-order polynomial fitting from original measurements along each satellite track. This procedure is applied to $[-60^\circ\ 60^\circ]$ latitude to avoid complications in the determination of wind direction in auroral regions. Although the density has no such complication, we limit it to the same latitude range to keep consistency.

Spatial scales of the residuals is between about 70–6000 km. The residuals are then classified into three seasons as combined equinox, June and December solstices. Combined equinox is used, because little difference has been found between March and September equinox during our analysis.

3. The terminator effect in the thermospheric zonal wind

Plots on the left-hand side of Figure 1 depict distributions of zonal wind residuals over latitude and local time. Taking June solstice as an example, we see a region of banded structures during 17–24 LT. Eastward and westward residual winds occur interchangeably in these bands, with a magnitude of about 5–15 m s^{-1} (corresponding to about 5-20% of the mean zonal wind velocity during this local time period). This wave-like structure closely resembles that in the thermospheric density shown in *Forbes et al.* [2008] and also in the next section in this paper. It extends from $\sim 40°$N to beyond $60°$S, intersecting the dusk terminator near 1930 LT at an angle of about $30°$. A rough estimation yields wavelengths in the range of 3000–4500 km, depending on which maximum is used. Although some wave signatures can be discerned on the dayside of the dusk terminator, most portion of the structure lies on the nightside. Contrasting to these pronounced wave-like structures at dusk, no similar tilted bands are discernible near the dawn terminator. During 00–06 LT, eastward residual wind above 10 m s^{-1} occurs near the equator, while westward residual wind with similar speed exists near $\pm 40°$ latitudes. These structures tend to stretch in the horizontal direction.

Figure 1

Wind distribution around December Solstice (the middle-left panel in Figure 1) shows salient features resembling those around June solstice, only with a reversed direction of the wavefront in the evening sector. But the inclination of the wavefront to the dusk terminator remains to be about $30°$. Similar to those near June solstice, tilted wave structures tend to extend further to higher latitude in winter hemisphere than in summer hemisphere. This may be simply due to the fact that the terminator line passes through higher latitude in winter hemisphere, though more complicated mechanisms might be involved as well.

Around equinoxes (the bottom-left panel of Figure 1), banded structures tilted from the terminator again form at dusk. However, bands in the northern and southern hemisphere apparently lie in different directions, unlike those around solstices. These titled wave structures are mainly confined to the pre-midnight sector. In postmidnight to morning sector, horizontally stretched structures are observed, similar to those near solstices. Their wavelengths (~ 6000 km) appear to be larger than that of the tilted waves near the dusk terminator.

Note that in all seasons around 20 LT, an eastward residual wind of 5–15 m s^{-1} is observed at the equator, sandwiched by westward residual wind of $-15 - -10$ m s^{-1} at about $\pm 25°$ latitude. Recall that the mean zonal wind is eastward about 150 m s^{-1} at 20 LT [*Liu et al.*, 2009], these residual winds indicate enhancement of the zonal wind at the equator, but abatement on both sides. This structure is consistent with the fast wind jet observed at the equator by CHAMP and DE2 [*Raghavarao et al.*, 1991; *Liu et al.*, 2009].

4. The terminator wave in the thermospheric density

Terminator waves in the thermospheric density have been shown by *Forbes et al.* [2008] using CHAMP data during the years of 2001–2007. For a better comparison with wave structures in zonal winds, here we have reanalyzed the density data during the corresponding period of 2002–2004.

Plots on the right-hand side of Figure 1 depict distributions of residual density over latitude and local time. These plots reveal salient features which resemble those shown in *Forbes et al.* [2008]. Tilted wave-like structures stand out prominently around solstices near the terminator, being more pronounced at dusk than at dawn. They are about $30°$ inclined to the terminator line at 0530LT and 1930 LT. The direction of wavefronts reverses from June solstice to December solstice along with the reverse of the terminator. The residual density amounts to values about $\pm 0.25 \times 10^{-12}$ kg m^{-3}, corresponding to about $\pm 6 - 8\%$ of the mean density on the nightside. Wave structures tend to extend further to high latitudes in winter hemisphere than in summer hemisphere. For instance, the band of negative residual density marked by white dashed lines near the dusk terminator around June solstice stretches from $30°$N to about $60°$S. On the dayside between 08–14 LT, two horizontal bands of positive residual show up prominently near $30°$N and $30°$S, with a band of negative residual density sitting at the equator. This structure is the well-known equatorial mass density anomaly (EMA) [*Liu et al.*, 2007].

The distribution of residual density around equinox (the bottom-right panel of Figure 1) shows bands of interchanging enhancements and depressions as well. They lie horizontally on the dayside, being the EMA noted above. On the nightside, the structure is tilted to the terminator. Although not as easily recognized as those near solstices, there seem to be two groups of fluctuation bands interfering with each other. Note that these tilted bands are mainly confined to the nightside of the terminator, regardless of season. Same features have been seen in the zonal wind residuals shown in previous section, which may signal easier propagation of these waves on the nightside due to smaller ion drag.

5. Discussion

The above analysis has revealed clear wave-like structures in both thermospheric zonal wind and density. Near the dusk solar terminator, this structure in the wind bears much similarity to that in the density. Both have wavefronts inclined to the terminator. Both have wavelengths of about 3000–4500 km. Both experience similar seasonal variation. This confirms our expectation in the introduction, in that the wind should also bear wave-like signatures near the terminator, given if the density does. In light of *Forbes et al.* [2008], these wave-like structures could well be excited by the moving solar terminator. They have several interesting characteristics, which we would like to discuss below.

First, although resembling each other, a prominent phase shift exists between the wave structures in the wind and density. One can notice this shift either by comparing locations of fluctuation bands in Figure 1, or by referring to Figure 2. In this figure, we have taken the case of June solstice as an example and plotted two cross-sections of the structure, one at a fixed local time (20 LT) and the other at a fixed latitude ($0°$N). It becomes immediately evident that the wind and density waves are phase-shifted to each other by somewhat more than $90°$. One reason for this phase shift could be the wind-density relationship via pressure gradient. In a structure of interchanging density maxima and minima, local perturbation wind will blow from a density maximum to a density minimum, while zero wind velocity is expected at the location of density maxima or minima. This consequently results in a phase shift between the density and wind structures, which would be $90°$ in an ideal case. Since our results are based on observations which are (1) averaged over many days and (2) only the zonal component of the wind,

Figure 2

the exact degree of the phase shift might have been smeared. But the phase-shift nature shows up unmistakably.

Second, wavefronts of both the wind and density wave structures exhibit a distinct rotation from the terminator. On the other hand, supposing these waves were excited by the moving solar terminator at the same altitude, we would naturally expect their wavefronts to be aligned with the terminator line. Although the multi-day averaging may somehow contribute it, this rotation is unlikely to be an artifact. This is because even the model simulation where no averages were done still produces a significant rotation as shown in *Forbes et al.* [2008]. Although we still do not have at our disposal a satisfactory explanation for the observed rotation, a reasonable conjecture is in favor of an coupling between the lower and upper atmosphere via upward wave propagation. As pointed out by *Fujiwara and Miyoshi* [2006], terminator wave structures in the thermosphere tend to disappear when neutral winds at lower altitude are set to zero in their model. This may well indicate that the terminator wave structure in the thermosphere is at least partly driven by the lower atmospheric variability, although its effects are largely damped by molecular diffusion, thermal conductivity and ion drag. The rotation of the wavefronts seen near 400 km could be an aggregate effect of the upward transmission of waves excited at lower altitude as speculated by *Forbes et al.* [2008]. Although possible interference of terminator waves with equatorward propagating large-scale gravity waves launched in auroral regions could not be excluded, its effect should be rather small during geomagnetic quiet conditions of Kp$\leq$3.

Furthermore, wave signatures show a clear dawn-dusk asymmetry, with more pronounced wave structures at dusk. This might suggest that the dusk terminator is more efficient in generating waves in the neutral atmosphere than the dawn terminator. As a boundary with inhomogeneous heating of the atmosphere, the dusk terminator bears in all seasons a larger temperature/pressure gradient than the dawn terminator as shown in Figure 3. According to theories [*Cot and Teitelbaum*, 1980; *Somsikov*, 1991], the sharper the boundary is, the more efficient it is as a wave-generating source. Thus, the dusk terminator works more effectively in exciting atmospheric waves. As to why terminator-wave signatures in dawnside zonal winds are indiscernible at all, our speculation is that the direction of zonal winds relative to the westward propagating terminator wave might have made the difference (zonal winds blow eastward along the dusk terminator, while westward or nearly zero along the dawn terminator [*Liu et al.*, 2009]), although exact mechanism is yet to be clarified. Other effects like strong longitudinal variation in the dawnside wind [*Häusler et al.*, 2007] might also have overridden the terminator effect. **Figure 3**

Finally, a local density maximum is seen in all seasons at the midnight equator (see right-hand side of Figure 1). This feature has been reported before and termed the Midnight Density Maximum (MDM) [*Arduini et al.*, 1997; *Liu et al.*, 2005]. In our present analysis, the MDM manifests itself as a feature closely related to the convergence of terminator wave crests on the dawn and dusk sides. When viewed in this context, the mechanism causing the MDM may be different from that suggested before based on ion-neutral momentum coupling with subsidence heating around the midnight equator [*Spencer et al.*, 1979]. Global-scale wave models should be used for investigating the role of terminator waves in generating the MDM.

Acknowledgments. The CHAMP mission is supported by the German Aerospace Center (DRL) in operation and by the Federal Ministry of Education and Research (BMBF) in data processing.

References

Arduini, C., G. Laneve, and F. A. Herrero (1997), Local time and altitude variation of equatorial thermosphere midnight denisty maximum (MDM): San Marco drag balance measurements, *Geophys. Res. Lett.*, *24*, 377–380.

Beer, T. (1973), Supersonic generation of atmospheric waves, *Nature*, *242*, 34.

Beer, T. (1978), On atmospheric wave generation by the terminator, *Planet. Space Sci.*, *26*, 185–188.

Cot, C., and H. Teitelbaum (1980), Generation of gravity waves by inhomogeneous heating of the atmosphere, *J. Atmos. Terr. Phys.*, *42*, 877–883.

Forbes, J. M., S. L. Bruinsma, Y. Miyoshi, and H. Fujiwara (2008), A solar terminator wave in thermosphere neutral densities measured by the CHAMP satellite, *Geophys. Res. Lett.*, *35*, L14802, doi:10.1029/2008GL034075.

Fujiwara, H., and Y. Miyoshi (2006), Characteristics of the large-scale traveling atmospheric disturbances during geomagnetically quiet and disturbed periods simulated by a whole atmosphere general circulation model, *Geophys. Res. Lett.*, L20108, doi:10.1029/2006GL027103.

Galushko, V. G., V. V. Paznukhov, Y. M. Yampolski, and J. C. Foster (1998), Incoherent scatter radar observations of agw/tid events generated by the moving solar terminator, *Ann. Geophys.*, *16*, 821–827.

Häusler, K., H. Lühr, S. Rentz, and W. Köhler (2007), A statistical analysis of longitudinal dependences of upper thermospheric zonal winds at dip equator latitudes derived from CHAMP, *J. Atmos. Solar-Terr. Phys.*, *69*, 1419–1430.

Hocke, K., and K. Igarashi (2002), Electron density in the f region derived from GPS/MET radio occultation data and comparison with IRI, *Earth Planets Space*, *54*, 947–954.

Liu, H., H. Lühr, V. Henize, and W. Köhler (2005), Global distribution of the thermospheric total mass density derived from CHAMP, *J. Geophys. Res.*, *110*, A04301, doi: 10.1029/2004JA010741.

Liu, H., H. Lühr, S. Watanabe, W. Köhler, V. Henize, and P. Visser (2006), Zonal winds in the equatorial upper thermosphere: decomposing the solar flux, geomagnetic activity, and seasonal dependencies, *J. Geophys. Res.*, *111*, A09S29, doi:10.1029/2005JA011415.

Liu, H., H. Lühr, and S. Watanabe (2007), Climatology of the Equatorial Mass Density Anomaly, *J. Geophys. Res.*, *112*, A05305, doi:10.1029/2006JA012199.

Liu, H., S. Watanabe, and T. Kondo (2009), Fast thermospheric wind jet at the Earth's dip equator, *Geophys. Res. Lett.*, *36*, doi:10.1029/2009GL037377, in press.

Raghavarao, R., L. E. Wharton, N. W. Spencer, H. G. Mayr, and L. H. Brace (1991), An equatorial temperature and wind anomaly (ETWA), *Geophys. Res. Lett.*, *18*(7), 1193–1196.

Somsikov, V. M. (1987), A spherical model of wave generation in the atmosphere by the solar terminator, *J. Atmos. Terr. Phys.*, *49*, 433–438.

Somsikov, V. M. (1991), Waves in the atmosphere due to the solar terminator, *Geomagn. Aeron.*, *31*, 1–8.

Somsikov, V. M. (1995), On the formation of atmospheric irregularities in the solar terminator region, *J. Atmos. Solar-Terr. Phys.*, *57*, 75–83.

Somsikov, V. M., and B. Ganguly (1995), On the formation of atmospheric inhomogeneities in the solar terminator region, *J. Atmos. Solar-Terr. Phys.*, *57*, 1513–1523.

Spencer, N. W., G. R. Carignan, H. G. Mayr, H. B. Niemann, R. F. Theis, and L. E. Wharton (1979), The midnight temperature maximum in the Earth's equatorial thermosphere, *Geophys. Res. Lett.*, *6*, 444–446.

Wharton, L. E., N. W. Spencer, and H. G. Mayr (1984), The earth's thermospheric superrotation from dynamics explorer 2, *Geophys. Res. Lett.*, *11*, 531–533.

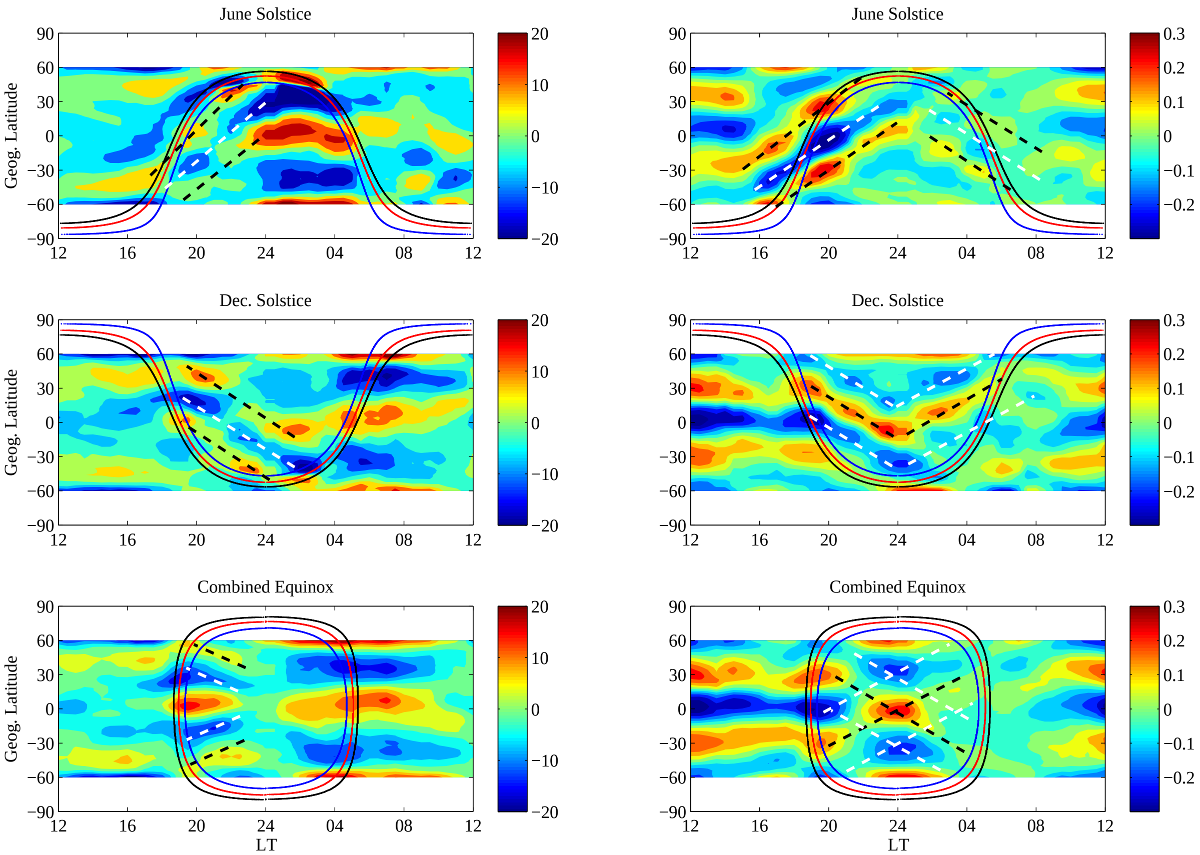

Figure 1. Distribution of residual zonal wind (left-hand side) and residual density (right-hand side) over latitude and local time. The residual zonal wind is in unit of m s^{-1}, and positive values mean eastward. The residual density is in unit of 10^{-12}kg m^{-3}. Solid lines depict the location of the solar terminator at three different altitudes: 100 km (black), 200 km (red), and 400 km (blue).

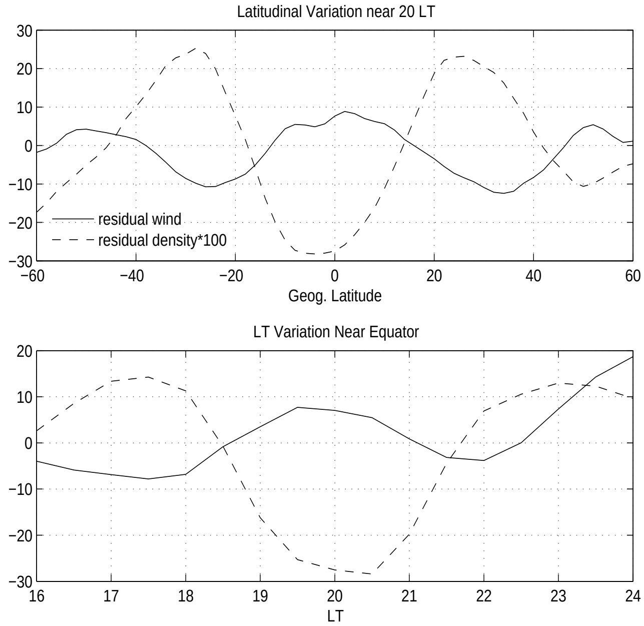

Figure 2. Cross-sections of the wave structures around June solstice at a fixed local time of 20 LT (upper) and at a fixed latitude of 15° N. The residual wind is in unit of m s^{-1} and the residual density is in unit of 10^{-10}kg m^{-3}. The residual density is plotted with a factor of 100 to facilitate easy comparison. Note that the residual density and wind are phase-shifted to each other.

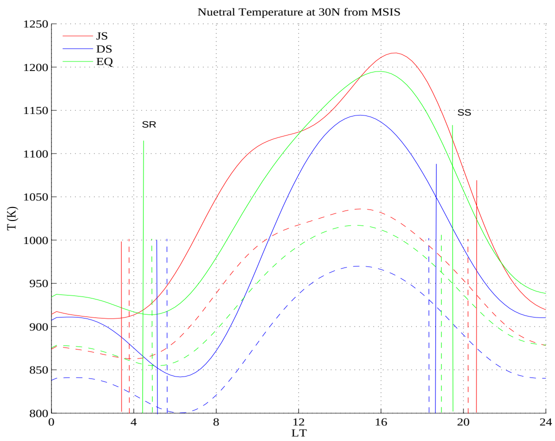

Figure 3. Diurnal variation of the neutral temperature at 30N geographic latitude in various seasons calculated from MSISE90 model. Solid lines are for 400 km altitude, and the dashed ones for 200 km altitude. Vertical lines denote corresponding time for sunrise and sunset. Note that at both heights, the temperature variation is sharper at dusk than at dawn.